

This article was downloaded by: [University of Haifa Library]

On: 17 August 2012, At: 10:21

Publisher: Taylor & Francis

Informa Ltd Registered in England and Wales Registered Number: 1072954

Registered office: Mortimer House, 37-41 Mortimer Street, London W1T 3JH, UK



Molecular Crystals and Liquid Crystals Science and Technology. Section A. Molecular Crystals and Liquid Crystals

Publication details, including instructions for authors and subscription information:

<http://www.tandfonline.com/loi/gmcl19>

Topology and Spin Polarization in Sheetlike Metal(II) Polymers: $[ML_2X_2]$ ($M = Mn, Fe, Co$ or Ni , $L =$ Pyrimidine or Pyrazine and $X = NCS$ or NCO)

Francesc Lloret^a, Miguel Julve^a, Juan Cano^a & Giovanni De Munno^b

^a Departament de Química Inorgànica, Facultat de Química de la, Universitat de València, Dr. Moliner 50, E-46100, Burjassot, València, (Spain)

^b Dipartimento di Chimica, Università degli Studi della Calabria., 87030, Arcavacata di Rende, Cosenza, (Italy)

Version of record first published: 24 Sep 2006

To cite this article: Francesc Lloret, Miguel Julve, Juan Cano & Giovanni De Munno (1999): Topology and Spin Polarization in Sheetlike Metal(II) Polymers: $[ML_2X_2]$ ($M = Mn, Fe, Co$ or Ni , $L =$ Pyrimidine or Pyrazine and $X = NCS$ or NCO), Molecular Crystals and Liquid Crystals Science and Technology. Section A. Molecular Crystals and Liquid Crystals, 334:1, 569-585

To link to this article: <http://dx.doi.org/10.1080/10587259908023352>

PLEASE SCROLL DOWN FOR ARTICLE

Full terms and conditions of use: <http://www.tandfonline.com/page/terms-and-conditions>

This article may be used for research, teaching, and private study purposes. Any substantial or systematic reproduction, redistribution, reselling, loan, sub-licensing, systematic supply, or distribution in any form to anyone is expressly forbidden.

The publisher does not give any warranty express or implied or make any representation that the contents will be complete or accurate or up to date. The accuracy of any instructions, formulae, and drug doses should be independently verified with primary sources. The publisher shall not be liable for any loss, actions, claims, proceedings, demand, or costs or damages whatsoever or howsoever caused arising directly or indirectly in connection with or arising out of the use of this material.

Topology and Spin Polarization in Sheetlike Metal(II) Polymers: $[ML_2X_2]$ ($M = Mn, Fe, Co$ or Ni , $L =$ Pyrimidine or Pyrazine and $X = NCS$ or NCO)

FRANCESC LLORET^a, MIGUEL JULVE^a, JUAN CANO^a and
GIOVANNI DE MUNNO^b

^a*Departament de Química Inorgànica, Facultat de Química de la Universitat de València. Dr. Moliner 50, E-46100 Burjassot, València (Spain) and* ^b*Dipartimento di Chimica, Università degli Studi della Calabria. 87030 Arcavacata di Rende, Cosenza (Italy)*

The preparation and the structural and magnetic characterization of a series of sheetlike transition metal polymers of formula $[ML_2X_2]$ [$M = Mn(II), Fe(II), Co(II)$ and $Ni(II)$; $L =$ pyrazine (pyz) and pyrimidine (pym); $X =$ pseudohalide anion] are presented herein. The nature of the intralayer magnetic interaction is discussed as a function of the topology of the bridging ligand. The results show that the spin polarization mechanism can be operative in these systems.

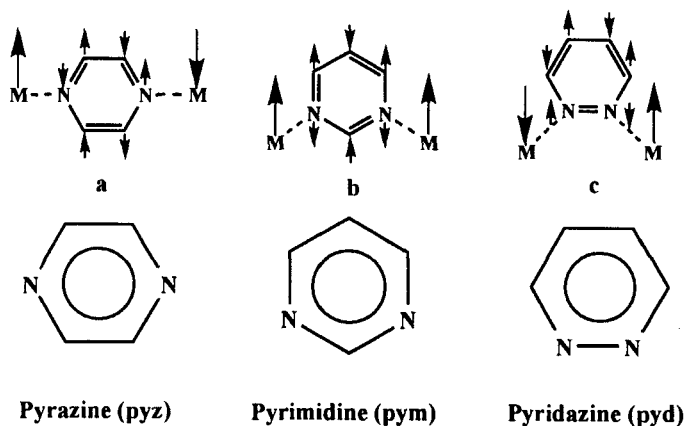
Keywords: Spin Polarization; molecular magnets; weak ferromagnetism; metal complexes; pyrimidine complexes

INTRODUCTION

In general, the magnetic interaction between two paramagnetic centers is antiferromagnetic in nature. However, if the interacting spins reside in orthogonal orbitals, the parallel alignment of spins is favoured. This orthogonality can be achieved by either geometrical or topological symmetry.

Geometrical symmetry has been successfully applied to bimetallic compounds¹ as well as to metal-radical systems.² Recently, the topological symmetry is being intensively used in designing high-spin organic polyradical species and the intramolecular spin alignment can be explained in terms of the spin polarization mechanism.³ This mechanism describes how an unpaired electron on one atom polarizes the electron cloud on the adjacent atom in the opposite sense. This would result in an alternation of the spin density of atoms in the bridge, and consequently the sign of the magnetic exchange parameter, J , should alternate as additional atoms appear in the bridging pathway (see scheme I).

In this way, oligo-carbenes or radicals linked with *m*-phenylenes showing a high-spin ground state have been designed and prepared.⁴ However, chemical reactivity arising from strong tendency of the unpaired electrons to react and to form covalent bonds suggests that stable high-spin organic materials can be expected to be hard to prepare. In contrast, transition metal ions are very stable spin carriers and in principle, they would be the best candidates for this purpose.



SCHEME I

Although the spin polarization was shown to be valid for some oxygen or nitrogen perturbed systems⁵ as well as for some organic radical-paramagnetic transition metal ion type systems,⁶ the limits of its application are unclear, especially for coordination compounds containing transition metal ions as the only spin sources. In fact, polymeric transition-metal complexes containing pyrimidine (pym) bridges have been designed as an approach to molecule-based ferromagnets,⁷ but the first reports on this topic are not conclusive because the magnetic interactions are weak and a structural determination is lacking.^{7,8}

In an attempt to verify the validity of the spin polarization mechanism on these systems, we have prepared the sheetlike polymeric compounds of formula $[ML_2X_2]$ ($M = \text{Mn(II)}$, Fe(II) , Co(II) ⁹ or Ni(II) ; $L = \text{pyrazine (pyz)}$ or pyrimidine (pym) ; $X = \text{SCN}^-$ or NCO^-) and we have studied their variable-temperature magnetic properties. The monomeric complex $[\text{Co}(\text{pyd})_4(\text{NCS})_2]$ ⁹ ($\text{pyd} = \text{pyridazine}$) has been also prepared and its magnetic properties have been used as a reference for the magnetic behaviour of the orbitally degenerated Co(II) octahedral complex. The results that we have obtained are the subject of the present contribution.

STRUCTURAL PROPERTIES

The crystal structure of $[\text{Co}(\text{pyz})_2(\text{NCS})_2]$ ¹⁰ (**1**) and $[\text{Co}(\text{pym})_2(\text{NCS})_2]$ (**2**) consists of parallel sheets of square arrays of cobalt atoms bridged by bismonodentate pyz (**1**) (Figure 1) or pym (**2**) (Figure 2) groups. The electroneutrality is achieved by two thiocyanate ligands occupying the axial positions. The cobalt atom is in a compressed octahedral environment with four long Co-N(L) [2.210(1) and 2.261(2) Å for **1** and **2**, respectively] and two short Co-N(NCS) bonds [2.047(2) (**1**) and 2.026(3) Å (**2**)]. The metal atoms in **1** and **2** are on a $2/m$ site, that is they lie on the inversion centre at the intersection of a reflection plane and on a two-fold axis perpendicular to it. The metal-metal separation through pym in **2** (6.361 Å) is significantly shorter than that through pyz in **1** (7.225 Å).

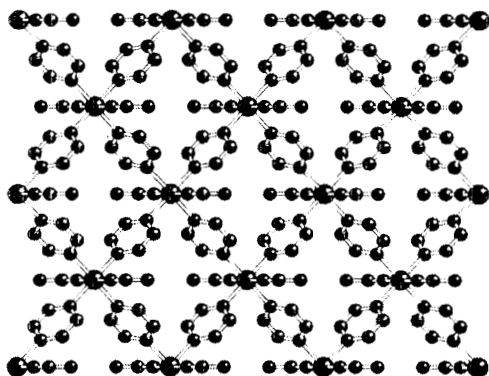


FIGURE 1: A section of the crystal structure of $[\text{Co}(\text{pyz})_2(\text{NCS})_2]$ (1)

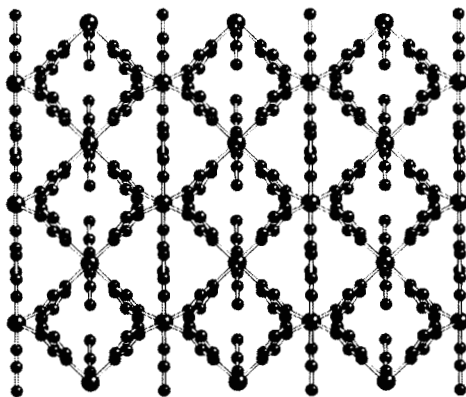


FIGURE 2: A section of the crystal structure of $[\text{Co}(\text{pym})_2(\text{NCS})_2]$ (2)

Considering a square unit of metal atoms within a sheet of **2**, the equatorial planes of opposite Co^{II} ions (constituted by four pyrimidine-nitrogens) are coplanar, whereas that of neighbouring metal ions form a dihedral angle of $80.7(1)^\circ$. The xz plane (sheet plane) forms dihedral angles of $40.4(1)$ and $90.0(1)^\circ$ with these equatorial planes and the mean pym plane, respectively. However, in the case of the related compound **1**, all the equatorial planes of the square unit (which are built by pyrazine-nitrogens) are coplanar and the values of the dihedral angles between the sheet plane (xy plane) and the equatorial and mean pyz planes are much reduced [$1.5(1)$ and $65.4(1)^\circ$, respectively]. Two adjacent sheets in **2** are separated by $8.487(2) \text{ \AA}$ (that is a $b/2$ translation), and they are shifted with respect to the other in such a way that the cobalt atoms of a sheet are located on the top of the centres of the square units of the other sheet. The distance between adjacent layers in **1** is 6.307 \AA and they are related by a translation of $a/3$ along the x axis. The shorter interlayer separation in **1** is due to the greater interpenetration between the sheets that it exhibits. This is impossible in the case of **2** in which the square units are more puckered and the pym rings are perpendicular to the sheet plane.

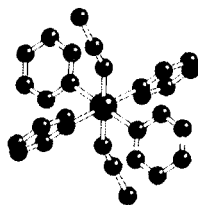


FIGURE 3: A perspective view of the structure of $[\text{Co}(\text{pyd})_4(\text{NCS})_2]$ (**3**)

The structure of $[\text{Co}(\text{pyd})_4(\text{SCN})_2]$ (**3**) is made up of neutral mononuclear units (Figure 3). The cobalt is in a compressed octahedral environment with four long Co-N(pyd) bonds [2.199(2)–2.261(2) Å] in the equatorial plane and two short axial Co-(NCS) bonds [2.057(2) Å], as in **1** and **2**. The pyd ligands are planar and the dihedral angle between the equatorial CoN_4 plane and the pyd planes are $50.3(1)^\circ$ and $120.3(1)^\circ$. The shortest intermolecular metal-metal separation is 7.769(3) Å.

Finally, as far as the compounds of formula $[\text{M}(\text{pyz})_2\text{X}_2]$ and $[\text{M}(\text{pym})_2\text{X}_2]$ ($\text{M} = \text{Mn}, \text{Fe}$ and Ni) are concerned, they are isostructural with **1** and **2**, respectively.

MAGNETIC PROPERTIES

Magnetic Properties of 1–3: The magnetic behaviour of compounds **1–3** is shown in Figure 4. At room-temperature, the χ_{MT} value (χ_{M} is the molar magnetic susceptibility per cobalt atom) is similar for all these compounds (χ_{MT} ca $3.3 \text{ cm}^3 \text{ K mol}^{-1}$) and it decreases upon cooling. This decrease is related to a spin-orbit coupling effect. In fact, their magnetic behaviour can be theoretically reproduced, in the temperature range 20–300 K, as monomeric octahedral Co^{II} complexes with λ (spin-orbit coupling parameter) = -126 cm^{-1} and k (orbital reduction parameter) = 0.75 (solid line in Figure 4). Complex **3** still follows this theoretical behaviour at low temperatures, whereas in the other two cases, χ_{MT} increases (**2**) and decreases (**1**) rapidly, indicating the presence of ferro- (**2**) and antiferromagnetic (**1**) interactions.

The temperature dependence of the molar magnetization, M , for **2** was investigated under an applied magnetic field $H = 70 \text{ G}$ (Figure 4, right). When the sample was cooled within the field, the field-cooled magnetization showed an abrupt break at 8.2 K. After cooling the sample in zero field and then warming it within the field, the zero-field-cooled magnetization had a maximum just below 8.2 K. All these features are characteristic of a magnetically ordered state existing below 8.2 K. The ordering temperature, T_{C} , was also confirmed by the measurement of both the in-phase, χ' , and out-

of-phase, χ'' , components of the *ac* magnetic susceptibility (inset of Figure 4 right).

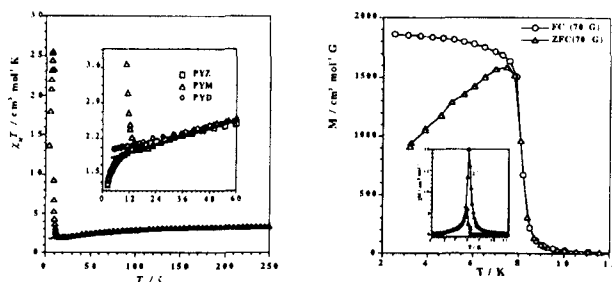


FIGURE 4: (Left) χ_M/T versus T plot for complexes **1** (O), **2** (Δ) and **3** (\square). (Right) The thermal dependence of the magnetization as a function of the applied field for **2**. The inset shows the thermal dependence of the in-phase, χ' , and out-of-phase, χ'' , components of the *ac* magnetic susceptibility.

The magnetic hysteresis loop for **2** was measured at 2.3 K (inset of Figure 5) and it showed to be characteristic of a soft magnet with a small coercive field of 120 G and a remnant magnetization of 0.25 N β . The M versus H plot at different temperatures (Figure 5) varied linearly up to the maximum field strength studied. The spontaneous magnetization extrapolated to $H = 0$ was 0.7 N β , which is only *ca* 15 % of the theoretical value (*ca* 4.3 N β). This feature is probably due to the occurrence of interlayer antiferromagnetic interactions leading to a spin canting structure between layers. Curiously, the curves present a first crossing point at *ca.* 25 kG and most likely, a second one at the highest value of the available magnetic field (7 T). This may be attributed to the weak interlayer antiferromagnetic interactions which are overcome by the applied field leading to a metamagnetic-like behaviour with a critical field close to 7 T (that is the value corresponding to the second crossing point in Figure 5).

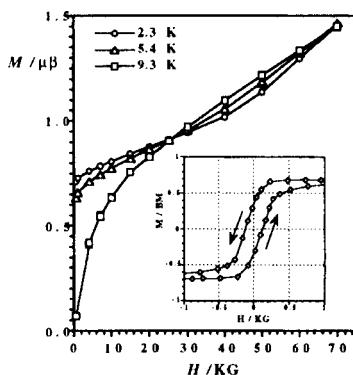


FIGURE 5: Magnetization against applied field for **2**. The inset shows the hysteresis loop at 2.3 K.

Magnetic Properties of [Co(pym)₂(NCO)₂](4**):** In order to analyze the influence of the interlayer magnetic interactions on the overall magnetic properties of these sheetlike polymers, we have replaced the thiocyanate by the cyanate group in compound **2**. The thermal dependence of $\chi_M T$ for **4** is similar to that of **2** (Figure 6, left), revealing the occurrence of an intralayer ferromagnetic interaction as in **2**. However, in contrast to **2**, a maximum of χ_M is observed at *ca* 4.2 K (for applied fields lower than 250 G) as shown in the inset of Figure 6 (left). The presence of this maximum is a clear indication that an antiferromagnetic interlayer interaction occurs. The peculiar magnetic properties of **4** at low temperatures are consistent with a metamagnetic behaviour. The temperature dependence of the magnetization, in the form of M/H , at various fields is shown in the inset of Figure 6 (left). For values of the applied field less than 290 G, the curves display a maximum which broadens as H is increased and finally disappears for $H > 290$ G, demonstrating that a field-induced transition from an antiferromagnetic to a ferromagnetic ground state occurs.

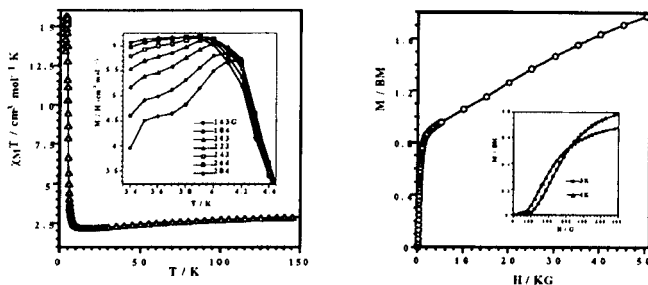


FIGURE 6: (Left) Variable-temperature $\chi_M T$ data for **4**. The inset shows the field-cooled magnetization (in the form of M/H) in different applied fields. (Right) Magnetization isotherms for **4**.

To confirm this metamagnetic behaviour, the magnetization vs applied field was measured at various temperatures (Figure 6, right). As the temperature is lowered, the isotherms become increasing sigmoidal and present a crossing point at *ca* 290 G, corresponding to the critical field. In the light of these results concerning the pym-bridged cobalt(II) polymers, one can describe them magnetically as ferromagnetic layers which interact each other in an antiferromagnetic fashion. For the thiocyanate derivative this antiferromagnetic interaction accounts for the spin canting structure (weak ferromagnet, $T_c = 8.5$ K) whereas for the cyanate one an antiferromagnet is formed ($T_c = 4.2$ K). This weak interlayer antiferromagnetic interaction can be easily broken by applied fields as low as 300 G allowing the description of **4** as a metamagnet.

Recently, Nakayama *et al.*¹¹ have investigated the magnetic properties of the related compounds of formula $[\text{Co}(\text{pym})_2\text{X}_2]$ ($\text{X} = \text{Cl}$ and Br). These compounds present a chiral three-dimensional structure through bridging pym ligand and in agreement with our magnetic results they exhibit a ferromagnetic transition below 5 K.

Magnetic Properties of $[M(\text{pyz})_2(\text{NCS})_2]$; $M = \text{Ni}$ (5), Fe (7), Mn (9) and $[M(\text{pym})_2(\text{NCS})_2]$; $M = \text{Ni}$ (6), Fe (8), Mn (10): The magnetic behaviour of compounds 5–10 is shown in Figures 7 and 8. In all these cases, it can be seen that the $\chi_M T$ value decreases as the temperature is lowered, indicating that an overall antiferromagnetic coupling is involved. In addition, a maximum of susceptibility is observed for 6, 7 and 8 at 10, 3.5 and 2.5 K, respectively.

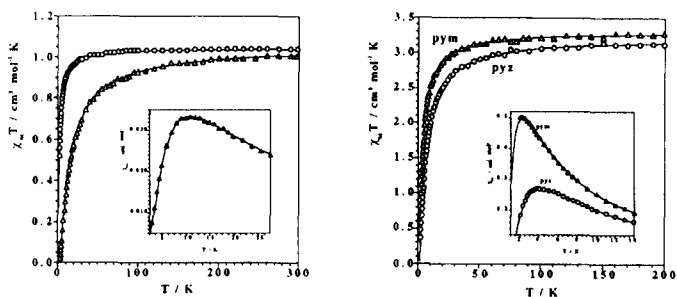


FIGURE 7: Thermal dependence of $\chi_M T$ for compounds 5 and 6 (left) and 7 and 8 (right). The inset shows the χ_M vs T plot.

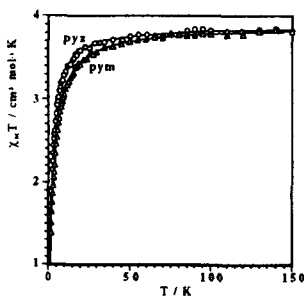


FIGURE 8: Thermal dependence of $\chi_M T$ for compounds 9 and 10.

We have determined the magnetic parameters J and g for this family of compounds by using the expressions proposed by Lines¹² for Heisenberg type square layers. A very good fit was obtained (solid line in Figures 7 and 8) and the values of the fitting parameters are listed in Table 1.

TABLE 1: Best-fit magnetic parameters for pyz- and pym-bridged metal complexes

Compound	g	J / cm^{-1}	$ n^2J $
[Ni(pyz) ₂ (NCS) ₂] 5	2.16	-0.8	3.2
[Ni(pym) ₂ (NCS) ₂] 6	2.17	-6.8	27.2
[Co(pyz) ₂ (NCS) ₂] 1	4.7	-1.0	9
[Co(pym) ₂ (NCS) ₂] 2	----	>0	----
[Co(pym) ₂ (NCO) ₂] 4	----	>0	----
[Fe(pyz) ₂ (NCS) ₂] 7	2.19	-0.9	14.4
[Fe(pym) ₂ (NCS) ₂] 8	2.22	-0.5	8.0
[Mn(pyz) ₂ (NCS) ₂] 9	1.99	-0.2	5.0
[Mn(pym) ₂ (NCS) ₂] 10	2.00	-0.3	7.5

DISCUSSION

The different metal centered magnetic orbitals involved in this family of complexes are shown in Figure 9. Assuming that the spin polarization mechanism is specially efficient through the π pathway, as observed in polycarbenes (orbital d_{xz} after the model system in Figure 9), we can attribute a ferromagnetic contribution for the d_{xz} magnetic orbital when pym acts as a bridging ligand (it should be antiferromagnetic for the case of bridging pyz). Antiferromagnetic contributions are predicted for the other magnetic orbitals due to the available superexchange mechanism.

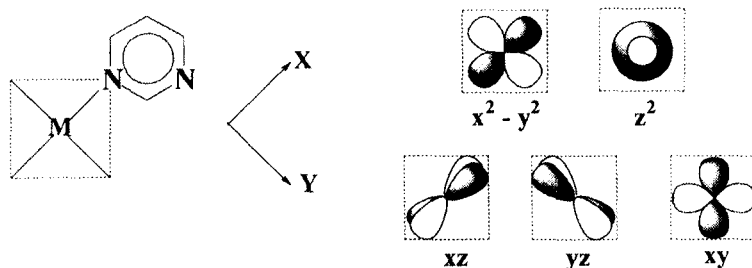


FIGURE 9: Magnetic orbitals involved in the pym-bridged compounds.

Keeping in mind that we are dealing with compressed octahedral coordination polyhedra, the electronic orbital splitting depicted in Figure 10 can be proposed. The stronger π -type interaction for the d_{xz} orbital respect to the d_{yz} one accounts for their non-degeneracy. In the light of Figures 9-10, one can see that only antiferromagnetic contributions are involved in the Ni(II) complexes. For the other metal ions one ferromagnetic contribution (d_{xz}) is always present but interestingly, the antiferromagnetic contributions increase when going from Co(II) to Mn(II). Consequently, the ferromagnetic coupling observed in the pym-bridged Co(II) complexes and the antiferromagnetic one in the analogous Ni(II) complex is not surprising if the spin polarization mechanism applies.

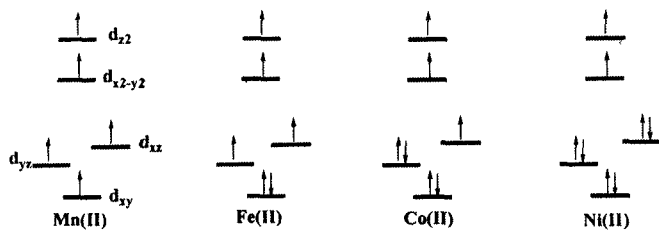


FIGURE 10: Orbital splitting in the compressed octahedral metal environment.

Because different number of magnetic orbitals are involved in this family, it is more appropriate to compare the values of n^2J instead of that of J (n being the number of magnetic orbitals). In general, this magnitude is not constant but it decreases when going from Ni(II) to Mn(II). This is true when among all the exchange pathway involved only one of them is predominant (the σ -pathway commonly). The irregular trend of the n^2J values in Table 1 for both pym and pyz families clearly shows the significant influence of the π pathway on the magnetic coupling. In addition, if all the magnetic contributions were antiferromagnetic, a larger antiferromagnetic coupling should be expected for the pym-bridged complexes, given that the number of atoms involved in the bridging skeleton of pyz is greater than that of pym. This is the actual situation for the Ni(II) complexes. The fact that the opposite trend is observed for the other metal complexes, strongly supports the occurrence of the ferromagnetic contribution attributed to the d_{xz} magnetic orbital in the pym derivatives which competes efficiently with the antiferromagnetic ones. To conclude, our feeling is that although the superexchange is always present, it is vanishing for extended bridging ligands and so, the spin polarization mechanism can be predominant. In this context the pym and pyz ligands behave as ferro- and antiferromagnetic linkers, respectively.

Molecular Orbital Considerations: The up-down-alternating spin polarization approach is a widely used tool to predict qualitatively the sign of the magnetic interaction. In this context, the bridging ligands sketched in I would lead to ferro- (Ib) and antiferromagnetic (Ia,c) couplings, in agreement with the experimental results. It is interesting to compare these predictions with those obtained through extended Hückel calculations. Figure 11 summarizes the results that we have obtained for vanadyl dinuclear compounds with bridging pyz (fig. 11a) and pym (fig 11b) ligands. The choice of the VO^{2+} cation with only one d_{xy} -type magnetic orbital interacting

via π , was aimed at simulating the π exchange pathway involved in the well known polycarbenes.

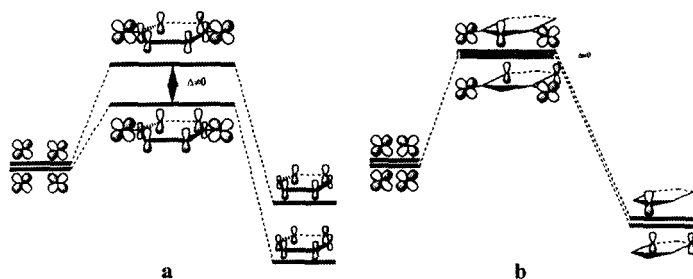
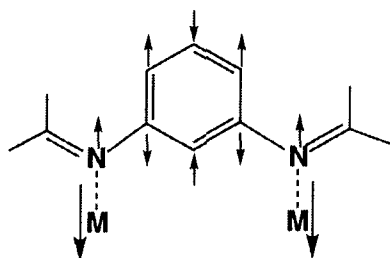


FIGURE 11: Molecular orbitals for pyz- (a) and pym- (b) bridged dinuclear vanadyl models.

The two HOMO's of pyz ligand which participate in the formation of the SOMO's have different bonding and antibonding contributions, and consequently they differ in energy. In addition, the two nitrogen atoms have significant electronic density and so, when they interact with the metallic fragments the corresponding SOMO's present a significant energy gap. In the case of the pym ligand, the corresponding HOMO's have neither bonding nor antibonding contributions, being thus degenerated. In addition, there is no electron density on the nitrogen atoms. So, degenerated SOMO's are obtained in their interaction with the metallic fragments. According to the Hay *et al.* model,¹³ antiferro- and ferromagnetic interactions are expected for the pyz- and pym-bridged compounds, respectively and in agreement with the spin-polarization predictions. It is interesting to note that ferromagnetic coupling has been observed for a pym-bridged vanadyle dinuclear compound.⁷

The same molecular orbital treatment carried out on the bridging ligand outlined in scheme II leads to the orbital picture shown in Figure 12. Although the HOMO's of the bridging ligand are degenerated, the occurrence of significant electron density on the nitrogen atoms and their different overlap intensity with the metallic fragments, causes an energy gap between

the SOMO's. An antiferromagnetic coupling is predicted for this system through the orbital model in contrast to the ferromagnetic coupling predicted by the up-down-alternating spin polarization rule.



SCHEME II

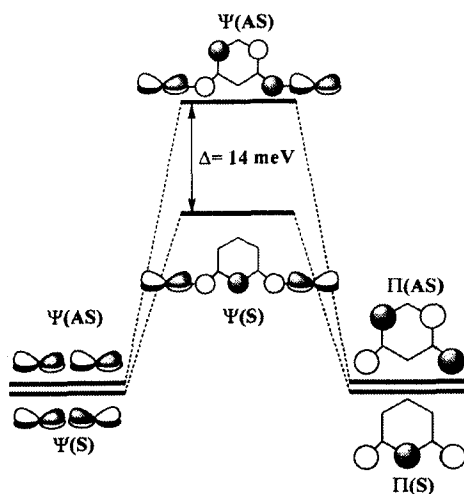
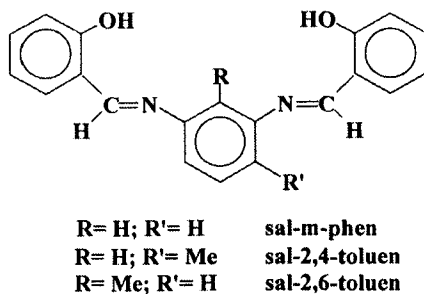


FIGURE 12: Molecular orbitals for the dinuclear vanadyl model with the bridging ligand sketched in III.

Recently¹⁴, some of us have investigated the magnetic properties of a series of dinuclear metal complexes of formula M_2L_2 ($M = \text{Cu(II)}, \text{Ni(II)}, \text{Co(II)}$ and Mn(II)) and L being the deprotonated form of the ligand sketched

in III). Their molecular structure is shown in Figure 13. In this family the metal ions present a tetrahedral surrounding and all these compounds exhibit intramolecular antiferromagnetic coupling. However, Oshio^{8a} has observed an intramolecular ferromagnetic coupling in an Fe(III) dinuclear complex with a bridging ligand with the same topology of III.



SCHEME III

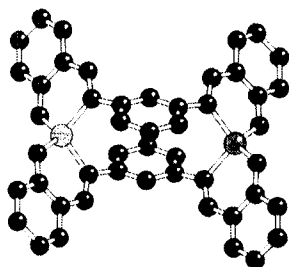


FIGURE 13: A perspective view of the molecular structure of $[M_2(\text{sal-}\mu\text{-phen})_2]$

All these results clearly show that further experimental and theoretical work is needed in order to provide a clearcut answer on the applicability of the spin polarization mechanism in exchange coupled coordination compounds.

Acknowledgments

This work was supported by the Spanish Dirección General de Investigación Científica y Técnica (DGICYT) (project PB97-1397) and the Italian Ministero dell'Università et della Ricerca Scientifica et Tecnologica and the TMR Programme from the European Union (Contract ERBFMRXCT98-0181).

References

- [1] O. Kahn, *Molecular Magnetism*, VCH Publishers, Inc., NY, (1993).
- [2] A. Caneschi, D. Gatteschi and R. Sesoli, *Acc. Chem. Res.*, **22**, 392, (1989).
- [3] (a) H.M. McConnell, *J. Chem. Phys.*, **39**, 1910, (1963); (b) N. Mataga, *Theor. Chim. Acta*, **10**, 372, (1968).
- [4] H. Iwamura, *Adv. Phys. Org. Chem.*, **26**, 179, (1990).
- [5] (a) F. Kanno, K. Inoue, N. Koga, H. Iwamura, *J. Phys. Chem.*, **97**, 13267, (1993); (b) M. Kitano, Y. Ishimaru, K. Inoue, N. Koga, H. Iwamura, *Inorg. Chem.*, **33**, 6012, (1994).
- [6] N. Koga, H. Ishimaru, H. Iwamura, *Angew. Chem., Int. Ed. Engl.* **108**, 815 (1996), and references therein.
- [7] T. Ishida and T. Nogami, *Recent Res Dev. Pure Applied Chem.*, **1**, (1997).
- [8] (a) H. Oshio, *J. Chem. Soc. Chem. Commun.*, 240, (1991); (b) A.M. W. Cargill Thompson, D. Gatteschi, J.A. McCleverty, J.A. Navas, E. Rentschler, M.D. Ward, *Inorg. Chem.*, **35**, 2701, (1996); (c) V.A. Ung, A.M.W. Cargill Thompson, D.A. Bardwell, D. Gatteschi, J.C. Jeffery, J.A. McCleverty, F. Totti, M.D. Ward, *Inorg. Chem.*, **36**, 3447, (1997).
- [9] F. Lloret, G. De Munno, M. Julve, J. Cano, R. Ruiz and A. Caneschi, *Angew. Chem. Int. Ed. Engl.*, **37**, 135, (1998).
- [10] The structure of **1** was published by J. Lu, T. Paliwala, S.C. Lim, C. Yu, T. Niu, A.J. Jacobson, *Inorg. Chem.*, **36**, 923, (1997) when we were writing the preceding paper. Due to the fact that our structural data of **1** fully agree with that reported we have kept only a few pertinent structural data of **1** for the sake of comparison with that of **2**.
- [11] K. Nakayama, T. Ishida, R. Takayama, D. Hashizume, M. Yasui, F. Iwasaki and T. Nogami, *Chem. Lett.*, 496, (1998).
- [12] J.E. Lines, *J. Phys. Chem. Solids*, **31**, 101, (1970).
- [13] P.J. Hay, J.C. Thibault and R. Hoffmann, *J. Am. Chem. Soc.*, **97**, 4884, (1975).
- [14] H. Hernández-Molina, A. Mederos, P. Gili, S. Domínguez, F. Lloret, J. Cano, M. Julve, C. Ruiz-Pérez and X. Solans, *J. Chem. Soc., Dalton Trans.*, 4327, (1997).